The current issue and full text archive of this journal is available on Emerald Insight at:
https://www.emerald.com/insight/2755-0907.htm

A constitutive model for cyclic densification of coarse-grained soil filler for the high-speed railway subgrade considering particle breakage

Received 10 January 2022
Revised 1 February 2022
Accepted 11 April 2022

Yangsheng Ye and Degou Cai
State Key Laboratory for Track Technology of High-Speed Railway, China Academy of Railway Sciences Corporation Limited, Beijing, China
Lin Geng
Beijing Tieke Special Engineering Technology Corporation Limited, China Academy of Railway Sciences Corporation Limited, Beijing, China, and
Hongye Yan, Junkai Yao and Feng Chen
State Key Laboratory for Track Technology of High-Speed Railway, China Academy of Railway Sciences Corporation Limited, Beijing, China

Abstract

Purpose – This study aims to propose a semiempirical and semitheoretical cyclic compaction constitutive model of coarse-grained soil filler for the high-speed railway (HSR) subgrade under cyclic load.

Design/methodology/approach – According to the basic framework of critical state soil mechanics and in view of the characteristics of the coarse-grained soil filler for the HSR subgrade to bear the train vibration load repeatedly for a long time, the hyperbolic empirical relationship between particle breakage and plastic work was derived. Considering the influence of cyclic vibration time and stress ratio, the particle breakage correction function of coarse-grained soil filler for the HSR subgrade under cyclic load was proposed. According to the classical theory of plastic mechanics, the shearing dilatation equation of the coarse-grained soil filler for the HSR subgrade considering particle breakage was modified and obtained. A semiempirical and semitheoretical cyclic compaction constitutive model of coarse-grained soil filler for the HSR subgrade under cyclic load was further established. The backward Euler method was used to discretize the constitutive equation, build a numerical algorithm of "elastic prediction and plastic modification" and make a secondary development of the program to solve the cyclic compaction model.

Findings – Through the comparison with the result of laboratory triaxial test under the cyclic loading of coarse-grained soil filler for the HSR subgrade, the accuracy and applicability of the cyclic compaction model were verified. Results show that the model can accurately predict the cumulative deformation characteristics of coarse-grained soil filler for the HSR subgrade under the train vibration loading repeatedly for a long time. It considers the effects of particle breakage and stress ratio, which can be used to calculate and analyze the stress and deformation evolution law of the subgrade structure for HSR.

© Yangsheng Ye, Degou Cai, Lin Geng, Hongye Yan, Junkai Yao and Feng Chen. Published in *Railway Sciences*. Published by Emerald Publishing Limited. This article is published under the Creative Commons Attribution (CC BY 4.0) licence. Anyone may reproduce, distribute, translate and create derivative works of this article (for both commercial and non-commercial purposes), subject to full attribution to the original publication and authors. The full terms of this licence may be seen at http://creativecommons.org/licences/by/4.0/legalcode

This research was supported by the National Natural Science Foundation of China [Grant No. 41731288 and 41972299], Task of Science and Technology R&D Program of China Railway Corporation [Grant No. P2018G050] and by the R&D Fund Project of China Academy of Railway Science Corporation Limited [Grant No. 2019YJ026]. On behalf all authors, the corresponding author states that there is no conflict of interest.

Railway Sciences
Vol. 1 No. 1, 2022
pp. 1-15
Emerald Publishing Limited
e-ISSN: 2755-0915
p-ISSN: 2755-0907
DOI 10.1108/RS-04-2022-0020

Originality/value – The research can provide a simple and practical method for calculating deformation of railway under cyclic loading.

Keywords High-speed railway, Subgrade, Coarse-grained soil filler, Particle breakage, Cumulative deformation, Stress ratio, Cyclic densification model

Paper type Research paper

1. Introduction

In recent years, the construction of high-speed railway (HSR) projects in China has ushered in vigorous development. By the end of 2019, China's HSR total mileage has registered 35,000 km and accounts for more than 60% of the HSR length throughout the world, ranking first worldwide. According to the *Medium- and Long-term Railway Network Planning* (Mid-term Adjustment in 2018), China will continue to build HSR on a certain scale in the future. However, the development of HSR in China has stepped into a long-term safe and stable operation stage from large-scale construction. The stable railway subgrade structural layer serves as a vital guarantee for the safe and smooth operation of HSR (Cai, Ye, Yan, Wei, & Yao, 2020).

Figure 1 shows a typical profile of ballastless track subgrade structure of HSR in China, which is mainly divided into surface layer of subgrade bed, bottom layer of subgrade bed and embankment body below subgrade bed (Tian, 2014b; Ye, Cai, Chen, Yang, & Chen, 2020a). Generally, the surface layer of subgrade bed is filled with graded crushed stones, featuring good engineering characteristics. The bottom layer of subgrade bed is filled with Groups A and B fillers, and the thickness of the bottom layer is 2.3 m, which generally accounts for more than half of the total height of the subgrade. Therefore, it is an important factor causing the deformation of the subgrade structure. In order to quantitatively describe the deformation characteristics of this subgrade structure under train load and evaluate the safety of subgrade operation in the future decades, it is necessary to establish a numerical calculation model, and choosing a suitable dynamic constitutive model is an important guarantee for the accuracy and reliability of numerical simulation results.

For laboratory tests, with the rapid development of large-scale indoor dynamic triaxial test equipment, many scholars have carried out a lot of research work on the dynamic characteristics of coarse-grained subgrade filler for HSR under cyclic loading (Hu, Wang, & Zhang, 2001; Tian, 2014a; Ning, 2018; Liu, Xie, Gao, & Zhan, 2013; Zhou *et al.*, 2016; Mei, Leng, Liu, Nie, & Xu, 2017; Zhang, Zhao, & Zhai, 2017; Bian, Jiang, Shen, & Chen, 2011; Wang, 2001). Physical and mechanical parameters related to the state of subgrade bed filler are tested and described in all aspects in these studies. The effects of different dynamic stress

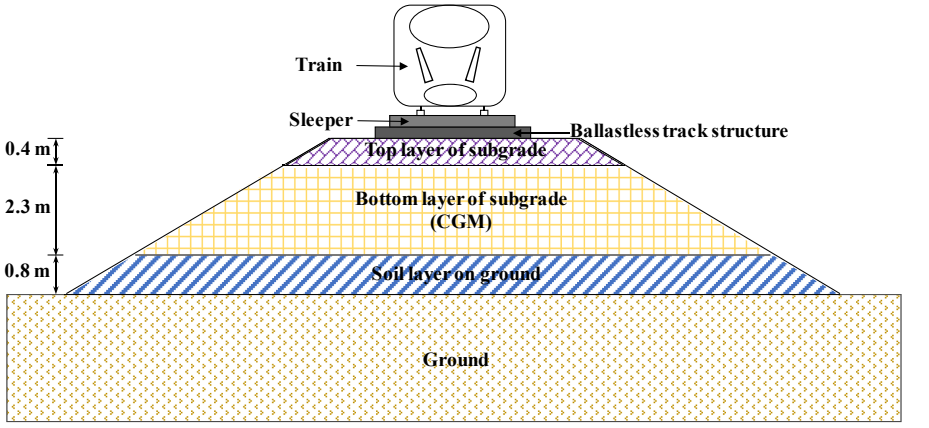

Figure 1.
Typical profile of ballastless track subgrade structure of HSR in China

amplitude, confining pressure and water content on the cumulative deformation of coarse-grained soil samples are studied. The evolution law of cumulative deformation with the cyclic loading vibration time is revealed, and the empirical expressions of the relationships between cumulative deformation and the cyclic vibration time, dynamic stress amplitude and confining pressure are established. However, these empirical models established based on the test results can only capture the cumulative deformation generated under each cyclic loading and cannot simulate the cyclic loading and unloading process during actual dynamic effect.

In terms of constitutive model, several dynamic constitutive models of soil have been developed so far. Equivalent linear model, a typical representative of viscoelastic model, was first proposed by Seed in 1968, which approximately considered the dynamic nonlinear property of soil by equivalent linearization method (Zhang & Ling, 2016). Hardin-Drnevich model (Hardin & Drnevich, 1972), Ramberg-Osgood model (Ramberg & Osgood, 1943), bilinear model and some combined curve models all belong to different forms of equivalent linearization models. Mroz first put forward the theory of plastic modulus field in 1967, which represented the beginning of the study on dynamic elastic–plastic model of soil (Morz, 1967). Iwan, Provest, Zienkie-wicz, Yang, Elgamal and others have established their own multi-yield surface models (Iwan, 1967; Provest, 1978; Zienkiewicz & Morz, 1984; Yang, Elgamal, & Parra, 2003). In China, Wang Jianhua, Xu Gancheng, Chen Shengshui and Zhuang Haiyang have established their own multi-yield surface models (Wang & Yao, 1994; Xu, Xie, & Zheng, 1995; Qiu & Zhang, 2011; Zhuang, Chen, & Zhu, 2006). Then, Dafalias and Popov (1975) proposed a more simplified boundary surface model based on Cambridge model. Tabbaa and Wood (1989) promoted the modified Cambridge model to a two-sided dynamic hardening model capable of describing the hysteretic response characteristics of clay under cyclic loading. However, the above-mentioned dynamic constitutive models generally have two problems: first, it can only simulate the situation where the number of cyclic loading is small (e.g. seismic load); second, grain crushing effect under cyclic loading is not considered.

Based on the constitutive theory of Indraratna, Thakur, Vinod and Salim (2012), the theory of critical state soil mechanics and classical plastic mechanics, in combination with the cyclic loading triaxial test, a constitutive model study on cyclic densification of coarse-grained soil filler in the HSR subgrade considering grain crushing is considered in this paper.

2. Deformation characteristics of coarse-grained soil filler for the HSR subgrade

2.1 Compactness

Under cyclic loading, the coarse-grained soil filler of HSR subgrade generally features nonlinearity, stress dependence, etc. Even when the stress level is very close to the static strength, the coarse-grained soil filler still shows strong compactness (Indraratna *et al.*, 2012; Ye *et al.*, 2020b). Under the initial loading conditions, the axial strain develops rapidly and partially rebounds during unloading, and each subsequent cyclic loading produces a continuous plastic strain increment. However, the amplitude of the plastic strain increment gradually decreases as the vibration load time increases. This is because the stiffness of coarse-grained soil filler becomes larger due to the previous stress under cyclic loading, and then the cumulative strain decreases under subsequent load. Under cyclic loading, the development of cumulative deformation of coarse-grained fillers of HSR subgrade is a gradual development process, and each single load will produce a small strain increment. A large number of dynamic triaxial tests show that the strain generated under the initial loading conditions is large, but the subsequent strain increments are continuously reduced under the premise that the stress amplitude and confining pressure remain unchanged, which is the compactness of coarse-grained fillers under cyclic loading. Deeply understanding and revealing this characteristic is conducive to guiding the research on the impact of vibration

load of roller during construction and high-speed train load during operation on compaction and vibration effect of coarse-grained subgrade fillers.

2.2 Crushing

Under static and dynamic loads, different degrees of grain crushing are generated for HSR coarse-grained subgrade filler. Hardin (1985) proposed to describe the crushing effect of coarse-grained soil filler under cyclic loading with relative grain crushing rate *Rr*, namely

$$R_r = \frac{S_{\mathrm{MPQ}}}{S_{\mathrm{MPN}}} \tag{1}$$

where S_{MPQ} is the total grain crushing degree, which is expressed by the area surrounded by the initial grading curve, the gradation curve after loading and the straight line with particle size equal to 0.075 mm in the gradation curve of coarse-grained soil filler for HSR subgrade before and after loading shown in Figure 2; S_{MPN} is the degree of potential grain crushing, which is expressed by the area surrounded by the initial gradation curve, 100% straight line and straight line with particle size equal to 0.075 mm in Figure 2.

3. Establishment of the cyclic densification model of coarse-grained soil filler for the HSR subgrade

3.1 Model assumption

The stress path of the coarse-grained soil filler for the HSR subgrade caused by cyclic triaxial loads under stress control conditions is shown in Figure 3. First, samples are subject to confining pressure and isotropically consolidated to the initial mean stress $\sigma_{p,0}$, then reaches the maximum mean stress $\sigma_{p,\max}$ (point B) under initial stress and then unloads to the minimum mean stress $\sigma_{p,\min}$ (point A). The subsequent loading and unloading events take place between points A and B along the path AB.

In order to establish the dynamic constitutive model of coarse-grained soil filler under cyclic loading in a simple and convenient manner, the following two assumptions are proposed.

(1) Under the initial loading conditions, the coarse-grained soil filler produces elastic–plastic deformation. The maximum stress state reached by the initial loading

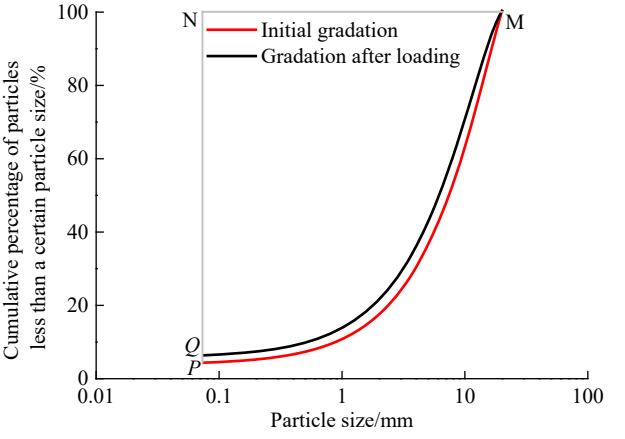

Figure 2.
Grading curve of coarse-grained soil filler for HSR subgrade before and after loading

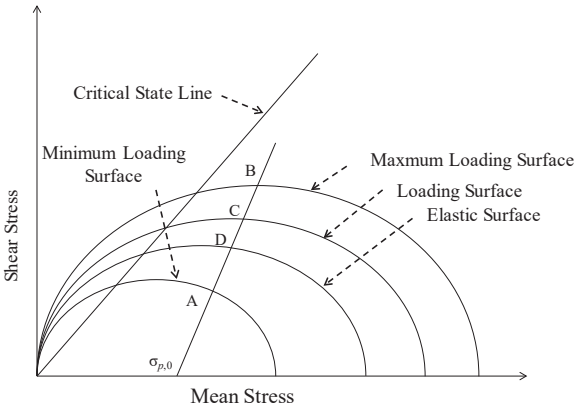

Figure 3.
Idealized stress path of coarse-grained subgrade filler under triaxial stress

condition is taken as the maximum loading surface under the current loading condition.

(2) There is one elastic surface that varies with the vibration time. The deformation outside the elastic surface is plastic deformation, while the deformation inside the elastic surface is regarded as elastic deformation.

3.2 Considering the shear dilatancy equation of grain crushing

Under triaxial stress, based on the principle of energy conservation, the following relationships of stress, strain and grain crushing can be obtained (Indraratna *et al.*, 2012).

$$\frac{\sigma_q}{\sigma_p} = \frac{\left(1-\frac{d\varepsilon_v}{d\varepsilon_1}\right)\tan^2\left(45^\circ+\frac{\varphi_f}{2}\right)-1}{\frac{2}{3}+\frac{1}{3}\left(1-\frac{d\varepsilon_v}{d\varepsilon_1}\right)\tan^2\left(45^\circ+\frac{\varphi_f}{2}\right)} + \frac{dE_B\left(1+\sin\varphi_f\right)}{\sigma_p d\varepsilon_1\left[\frac{2}{3}+\frac{1}{3}\left(1-\frac{d\varepsilon_v}{d\varepsilon_1}\right)\tan^2\left(45^\circ+\frac{\varphi_f}{2}\right)\right]} \tag{2}$$

where σ_q and σ_p are deviatoric stress and mean stress, respectively; $d\varepsilon_v$ and $d\varepsilon_1$ are the increments of axial strain and volume strain, respectively; φ_f is the basic friction angle; E_B is the energy consumed per unit volume of grain crushing.

According to the study in Jia, Xu, Chi, Xiang and Zhou (2017), E_B can be expressed by plastic work W_p per unit volume, while R_r has a hyperbolic relationship with W_p, namely

$$R_r = \frac{W_p}{a+bW_p} \tag{3}$$

where a and b are empirical parameters.

For the indoor triaxial test of coarse-grained soil filler of HSR subgrade under cyclic loading, W_{p} can be calculated by the area enclosed by the hysteretic curve, and then the R_{r} under cyclic loading can be obtained by Formula (3). Then, W_p and R_{r} are corresponding to the cumulative deformation one by one, and finally the relative grain crushing rate $\frac{dW_p}{d\varepsilon_1}$ and the plastic work consumption rate $\frac{dR_r}{d\varepsilon_1}$ per unit volume can be obtained, respectively, which can be expressed by linear relationship (Indraratna *et al.*, 2012) as

$$\frac{dW_p}{d\varepsilon_1} = \beta\frac{dR_r}{d\varepsilon_1} \tag{4}$$

where β is the empirical parameter.

Therefore, in combination with the expression forms of stress invariant and strain invariant, formula (2) can be rewritten as follows:

$$\frac{d\varepsilon_{v,p}}{d\varepsilon_{s,p}} = \frac{9(\eta_M - \eta_i)}{9 + 3\eta_M - 2\eta_i\eta_M} + \frac{\beta dR_r}{\sigma_p d\varepsilon_{s,p}} \frac{9\eta_M - 3}{9 + 3\eta_M - 2\eta_i\eta_M} \frac{6 + 4\eta_M}{6 + \eta_M} \tag{5}$$

where $d\varepsilon_{s,p}$ and $d\varepsilon_{v,p}$ are plastic body strain and shear strain increments respectively; ηM is the critical state stress ratio; η_i is the current stress ratio.

In actual engineering, the coarse-grained soil filler of HSR subgrade is affected by many factors. The cyclic stress ratio η_c and the vibration time N having a significant impact on the material performance are adopted as the influencing factors, and the influence on the grain crushing rate $\frac{dR_r}{d\varepsilon_1}$ is considered. In order to describe the loading and unloading amplitude of vibration load under different working conditions, a multiplier $\ln\frac{\sigma_{p,\max}}{\sigma_{p,\min}}$ is introduced to establish the evolution function of grain crushing rate with strain development, namely

$$\frac{dR_r}{d\varepsilon_1} = \frac{f_{\mathrm{SR}} f_N}{\ln\frac{\sigma_{p,\max}}{\sigma_{p,\min}}} \tag{6}$$

where f_{SR} and $\mathrm{f_N}$ are the correction functions of the influence of cyclic stress ratio and cyclic vibration time on grain crushing rate, respectively.

In $\sigma_q - \sigma_p$ stress space, according to the relationship $\varepsilon_{s,p} = \frac{2}{3}(\varepsilon_1 - \varepsilon_3)$ between shear strain $\varepsilon_{s,p}$ and axial strain ε_1 and radial strain ε_3 under axisymmetric stress and taking the Poisson's ratio of 0.3, $\varepsilon_1 = 1.15\,\varepsilon_{s,p}$ can be obtained, in combination with formula (6) and substituted into formula (5), obtaining

$$\frac{d\varepsilon_{v,p}}{d\varepsilon_{s,p}} = \frac{9(\eta_M - \eta_i)}{9 + 3\eta_M - 2\eta_i\eta_M} + \frac{\beta}{\sigma_p} \frac{1.15 f_{\mathrm{SR}} f_N}{\ln\frac{\sigma_{p,\max}}{\sigma_{p,\min}}} \frac{9\eta_M - 3}{9 + 3\eta_M - 2\eta_i\eta_M} \frac{6 + 4\eta_M}{6 + \eta_M} \tag{7}$$

Considering some constant parameters in formula (7), for the convenience of subsequent expression, formula (7) is rewritten as

$$\frac{d\varepsilon_{v,p}}{d\varepsilon_{s,p}} = \frac{9(\eta_M - \eta_i)}{9 + 3\eta_M - 2\eta_i\eta_M} + \frac{A f_{\mathrm{SR}} f_N}{\sigma_p(9 + 3\eta_M - 2\eta_i\eta_M)} \tag{8}$$

where

$$A = \frac{1.15\beta}{\ln\frac{\sigma_{p,\max}}{\sigma_{p,\min}}} \frac{(9 - 3\eta_M)(6 + 4\eta_M)}{6 + \eta_M}$$

Formula (8) is the shear dilatancy equation of coarse-grained soil filler under cyclic loading considering the grain crushing effect.

3.3 Incremental expression form of constitutive equation

In order to accurately describe the cumulative deformation characteristics and to facilitate numerical programming, the classical elastic–plastic theory often decomposes the total strain vector $\boldsymbol{\varepsilon}$ into

$$\boldsymbol{\varepsilon} = \boldsymbol{\varepsilon_e} + \boldsymbol{\varepsilon_p} \tag{9}$$

where ε_e and ε_p are elastic strain vectors and plastic strain vectors, respectively.

The increment form of the above formula can be written as

$$d\boldsymbol{\varepsilon} = d\boldsymbol{\varepsilon}_e + d\boldsymbol{\varepsilon}_p \tag{10}$$

where $d\varepsilon$, $d\varepsilon_e$ and $d\varepsilon_p$ are the total strain increment vector, the elastic strain increment vector and the plastic strain increment vector, respectively.

Similarly, for the strain invariants corresponding to the $\sigma_q - \sigma_p$ stress space, the shear strain increment $d\varepsilon_s$ and volume strain increment $d\varepsilon_v$ can be written as

$$d\varepsilon_s = d\varepsilon_{s,e} + d\varepsilon_{s,p} \tag{11}$$

$$d\varepsilon_v = d\varepsilon_{v,e} + d\varepsilon_{v,p} \tag{12}$$

where $d\varepsilon_{s,e}$, $d\varepsilon_{s,p}$, $d\varepsilon_{v,e}$, and $d\varepsilon_{v,p}$ are elastic shear strain increment, plastic shear strain increment, elastic volume strain increment and plastic volume strain increment, respectively.

In the elastic range, $d\varepsilon_{s,e}$ and $d\varepsilon_{v,e}$ can be calculated by the following formulas, respectively.

$$d\varepsilon_{s,e} = \frac{d\sigma_q}{3G} \tag{13}$$

$$d\varepsilon_{v,e} = \frac{\kappa}{1+e_i}\frac{d\sigma_p}{\sigma_p} \tag{14}$$

where e_i is the initial void ratio at the beginning of shear; G is the shear modulus and k is the slope of the rebound curve of the isotropic compression rebound test.

The strain vector for the plastic phase can be obtained from the following formula (Indraratna *et al.*, 2012).

$$d\boldsymbol{\varepsilon} = f_h \frac{\partial f_g}{\partial \boldsymbol{\sigma}} df_f \tag{15}$$

where f_h, f_g and f_f are the hardening function, the plastic potential function and the yield function, respectively.

3.4 Plastic potential function

In σ_q–σ_p stress space, the direction of the plastic strain increment is perpendicular to the plastic potential surface, so

$$\frac{d\varepsilon_{v,p}}{d\varepsilon_{s,p}} = -\frac{d\sigma_q}{d\sigma_p} \tag{16}$$

Put formula (16) into formula (8), we can get

$$\frac{d\sigma_q}{d\sigma_p} + \frac{9\sigma_p(\eta_M - \eta_i) + Af_{SR}f_N}{\sigma_p(9 + 3\eta_M - 2\eta_i\eta_M)} = 0 \tag{17}$$

It is not difficult to find out that the solution of formula (17) is the plastic potential function. However, it can be seen from formula (15) that precise plastic potential function is not required, but only partial differential forms of plastic potential function for σ_q and σ_p are required. With reference to the simplified calculation method in Indraratna *et al.* (2012), partial derivatives of plastic potential function for partial stress σ_q and mean stress σ_p are obtained, respectively:

$$\frac{\partial f_g}{\partial \sigma_q} = 1 \tag{18}$$

$$\frac{\partial f_g}{\partial \sigma_p} = \frac{9\sigma_p(\eta_M - \eta_i) + Af_{SR}f_N}{\sigma_p(9 + 3\eta_M - 2\eta_i\eta_M)} \tag{19}$$

3.5 Yield function

In this paper, the model only considers the plastic deformation of coarse-grained soil filler of HSR subgrade caused by shear stress, while the influence of hydrostatic pressure on plastic deformation of fillers is ignored. In $\sigma_q - \sigma_p$ stress space, the yield function f_f can be expressed as follows:

$$f_f = \sigma_q - \eta_i \sigma_p \tag{20}$$

When the loading path of cyclic loading coincides with the yield function, i.e. the yield function is 0, the material yield occurs, which is characterized by plastic deformation.

3.6 Plastic strain calculation under initial loading conditions

Using formula (15)–(20) and in combination with the method proposed by Indraratna and Salim to derive the hardening function from undrained stress conditions (Salim & Indraratna, 2004), the plastic strain under initial loading conditions can be obtained as follows:

$$d\varepsilon_{s.p} = \frac{2\alpha\kappa \frac{\sigma_p}{\sigma_{p,cs}} \left(1 - \frac{\sigma_{p,cu0(i)}}{\sigma_{p,cs(i)}}\right)(9 + 3\eta_M - 2\eta_M\eta_i)\eta_i d\eta_i}{\eta_M^2(1+e_i)\left(2\frac{\sigma_{p,cu0}}{\sigma_p} - 1\right)\left[9(\eta_M - \eta_i) + \frac{A}{\sigma_p}(f_{SR}f_N)\right]} \tag{21}$$

where a is the parameter related to the initial stiffness of coarse-grained subgrade filler; $\sigma_{p,cu0}$ and $\sigma_{p,cs}$ are the stresses at the intersection of the starting point of the undrained stress path and the critical state line in the current stress state; $\sigma_{p,cu0(i)}$ and $\sigma_{p,cs(i)}$ are the initial values of $\sigma_{p,cu0}$ and $\sigma_{p,cs}$ at the moment of loading under stress.

Since the current stress ratio may approach the critical stress ratio under low confining pressure, which will lead to a larger shear strain increment value, according to Indraratna *et al.* (2012), $\eta_i^* = \eta_i\left(\frac{\sigma_p}{\sigma_{p,cs}}\right)$ instead of η_i, so that the value of stress ratio in numerical calculation can be greater than the critical stress ratio, thus ensuring the stability and robustness of numerical calculation. According to Indraratna *et al.* (2012), formulas (21) and (8) can be rewritten as

$$d\varepsilon_{s.p} = \frac{2\alpha\kappa \frac{\sigma_p}{\sigma_{p,cs}} \left(1 - \frac{\sigma_{p,cu0(i)}}{\sigma_{p,cs(i)}}\right)(9 + 3\eta_M - 2\eta_M\eta_i^*)\eta_i d\eta_i}{\eta_M^2(1+e_i)\left(2\frac{\sigma_{p,cu0}}{\sigma_p} - 1\right)\left[9(\eta_M - \eta_i^*) + \frac{A}{\sigma_p}(f_{SR}f_N)\right]} \tag{22}$$

$$\frac{d\varepsilon_{v.p}}{d\varepsilon_{s.p}} = \frac{9(\eta_M - \eta_i)}{9 + 3\eta_M - 2\eta_i^*\eta_M} + \frac{Af_{SR}f_N}{\sigma_p(9 + 3\eta_M - 2\eta_i^*\eta_M)} \tag{23}$$

3.7 Plastic strain calculation under subsequent loading conditions

As above mentioned in this paper, under cyclic loading, the first loading of coarse-grained soil filler of HSR subgrade generates the maximum strain, and the cumulative deformation gradually tends to be stable with the increase of vibration times, namely, showing compactness. From the perspective of mathematical expression of constitutive equation, parameters representing material rigidity can be modified to simulate the compactness of subgrade filler. Therefore, the stiffness in the plastic strain formula under initial loading condition is modified, and a new plastic shear strain increment formula under the subsequent loading condition is obtained:

$$d\varepsilon_{s.p} = \alpha_1\alpha_2\alpha_3 \frac{2\alpha\kappa \frac{\sigma_p}{\sigma_{p,cs}} \left(1 - \frac{\sigma_{p,cu0(i)}}{\sigma_{p,cs(i)}}\right)(9 + 3\eta_M - 2\eta_M\eta_i^*)\eta_i d\eta_i}{\eta_M^2(1+e_i)\left(\frac{2\sigma_{p,cu0}}{\sigma_p} - 1\right)\left[9(\eta_M - \eta_i^*) + \frac{A}{\sigma_p}(f_{SR}f_N)\right]} \tag{24}$$

where

$$\alpha_1 = \begin{cases} \dfrac{\|AC\| - \|AD\|}{\|AB\|}, & \sigma_p > \sigma_{p,e} \\ \alpha_1 = 0, & \sigma_p \le \sigma_{p,e} \end{cases}$$

$$\alpha_2 = 1 - \frac{\eta_i^*}{\eta_M}$$

$$\alpha_3 = \frac{\mu}{N^\delta}$$

where α_1 is the parameter considering kinematic hardening effect; α_2 is a parameter considering the influence of subsequent loading stress ratio; α_3 is a parameter considering the influence of vibration times; μ and δ are model empirical constants related to cyclic vibration times; ||AB||, ||AC|| and ||AD|| are the distances between two points in the stress space of $\sigma_q - \sigma_p$ (see Figure 3); $\sigma_{p,e}$ is the elastic average stress (corresponding to point D in Figure 3).

α_1 is introduced to accurately simulate the Bauschinger effect. Since the material is elastic after a certain number of vibrations, an elastic surface is introduced to describe the effect of the loading history. The elastic surface hardens with the increase of vibration. However, $\sigma_{p,e}$ change in the given stress path AB, and the relationship between $\sigma_{p,e}$ and vibration time N given (Indraratna *et al.*, 2012) is

$$\sigma_{p,e} = \sigma_{p,\min} + \left(1 - \frac{1}{\ln(10+N)}\right)(\sigma_{p,\max} - \sigma_{p,\min}) \tag{25}$$

In Figure 3, point D is used to control the deformation of the material under subsequent loading conditions, and point C represents the current stress position. If C is higher than D, the material shows elastoplasticity, otherwise, the material shows elasticity.

α_2 is introduced to simulate the effect of the magnitude of stress ratio. When the filler is subjected to greater stress, namely, the closer the stress ratio is to the critical stress ratio, the greater the stiffness of the filler and the smaller the deformation.

α_3 is introduced to simulate the influence of cyclic vibration times. It is a function related to vibration times N. With the increase of loading times, the parameter α_3 gradually increases, which further reflects the increase of stiffness of the filler and the decrease of cumulative deformation.

After the shear strain is calculated by the above formulas, the plastic volume strain increment can be calculated by formula (24). Finally, the total shear strain and volume strain increments can be calculated by formulas (11) and (12).

4. Implementation of the cyclic densification model of coarse-grained soil filler for the HSR subgrade in the ABAQUS procedure

4.1 Numerical implementation process of cyclic densification model

The ABAQUS is a piece of finite element software, with a wide application range and powerful functions. It can simulate various problems from simple linear to complex nonlinear, which only provides standard finite element analysis program, but also has good openness. Users can develop user subprogram interface and application program interface with the help of the secondary development platform so as to expand the function of the master program and widely apply in the actual engineering (Cao, 2014). This paper adopts FORTRAN language to prepare a UMAT subprogram of cyclic densification model of coarse-grained soil filler for the HSR subgrade based on the secondary development interface of ABAQUS. The main process of UMAT subprogram is shown in Figure 4.

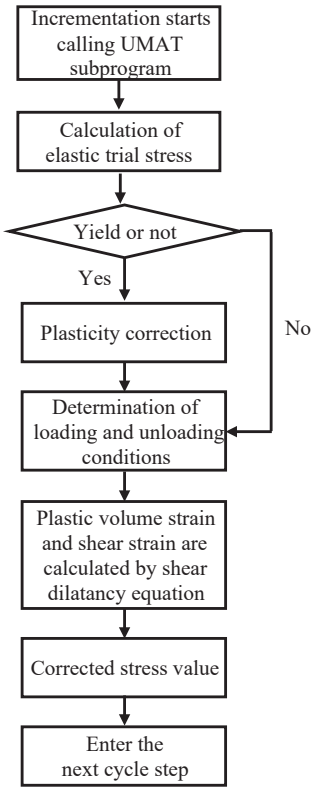

Figure 4.
Numerical implementation process of cyclic densification model

4.2 Numerical implementation and verification of the cyclic densification model

Based on the above description of the cyclic densification model and finite element numerical implementation method, two-dimensional symmetry method is adopted, and the finite element subprogram is prepared to predict the triaxial test results of coarse-grained subgrade filler.

Figure 5 is a schematic diagram of numerical simulation of the cyclic triaxial test. For convenience, the two-dimensional plane of the cylindrical triaxial sample is simulated, i.e. the dash area of the triaxial sample in Figure 5(a), and the two-dimensional eight-node in ABAQUS is used for quadratic-reduced integration unit; Figure 5(b) shows the mesh division and boundary conditions of the ABAQUS model. The left boundary of the model is the central axis, without lateral deformation. The lower boundary of the model restrains vertical and radial deformation. The top of the model is fixed radially, but free deformation is allowed in the vertical direction. The triaxial test process of cyclic loading is simulated with two analysis steps: first, defining the model boundary and confining pressure; second, applying vertical cyclic loading to the model.

In this paper, numerical calculation is carried out for triaxial test of coarse-grained soil under cyclic loading in Bian *et al.* (2016) and Tian *et al.* (2019). In numerical calculation, the model parameters are taken as follows.

According to the indoor vibration and compaction test results, the relation curve between the relative grain crushing rate and the plastic work per unit volume is drawn, as shown in Figure 6. Formula (3) is used to fit the test results, and the empirical parameters a and b of the coarse-grained soil filler of the HSR subgrade are equal to 1,855 and 0.083, respectively.

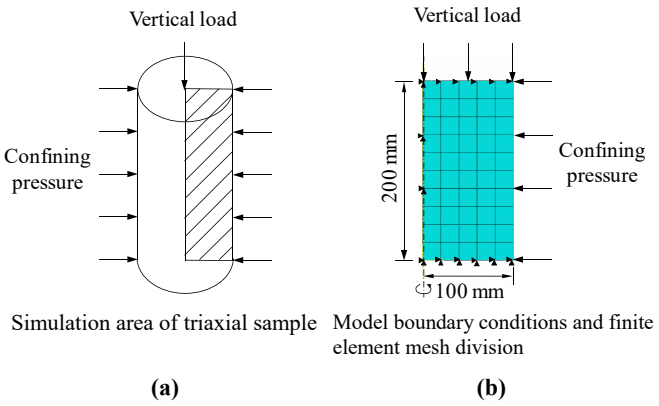

Figure 5.
Numerical model of cyclic triaxial test

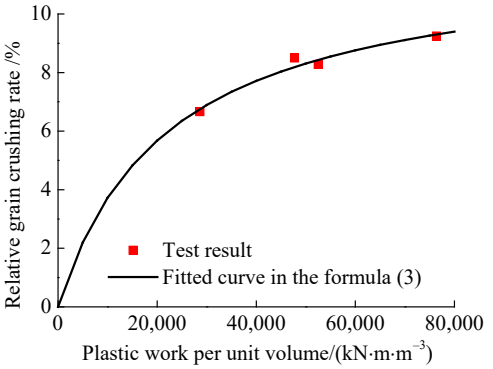

Figure 6.
Relationship between relative grain crushing rate and plastic work per unit volume

The hysteresis loop area enclosed by the stress–strain curve obtained by triaxial test under cyclic loading is used to calculate W_p, and the parameters a and b determined above are used to calculate R_r under cyclic loading. Then, W_p and R_r are corresponding to the cumulative deformation, and finally, the relative grain crushing rate $\frac{dR_r}{d\epsilon_1}$ and the energy consumption rate per unit volume $\frac{dW_p}{d\epsilon_1}$ are obtained, respectively, as shown in Figure 7. It can be seen from Figure 7 that linear relation is shown between the two, and the empirical parameter β obtained by fitting equals to 1,855.

According to the triaxial test results in Tian *et al.* (2019), the relationship between the f_{SR} and the cycle stress ratio and between the f_N and the cyclic vibration times can be obtained, as shown in Figure 8. Based on the least square method principle, the empirical expressions of f_{SR} and f_N are obtained by fitting

$$f_{SR} = C_{SR1}\eta_c^{C_{SR2}} + C_{SR3} \tag{26}$$

$$f_N = C_{N1}N^{C_{N2}} + C_{N3} \tag{27}$$

where $\eta_c = \frac{\sigma_d}{2\sigma_3}$, σ_d is the vertical dynamic stress amplitude of the triaxial test; σ_3 is the confining pressure of triaxial test; C_{SR1}, C_{SR2}, C_{SR3}, C_{N1}, C_{N2} and C_{N3} are the fitting parameters.

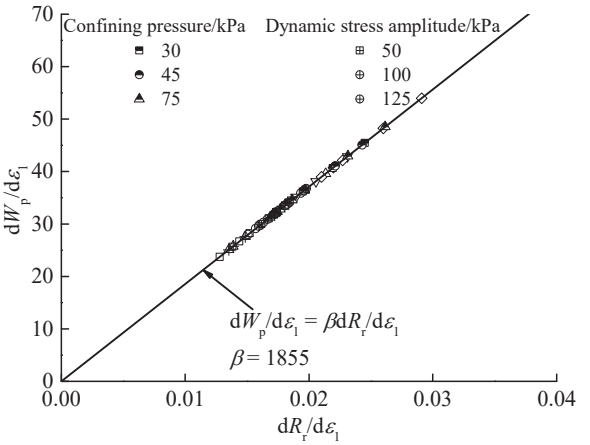

Figure 7.
Relationship between relative grain crushing rate and energy consumption rate per unit volume

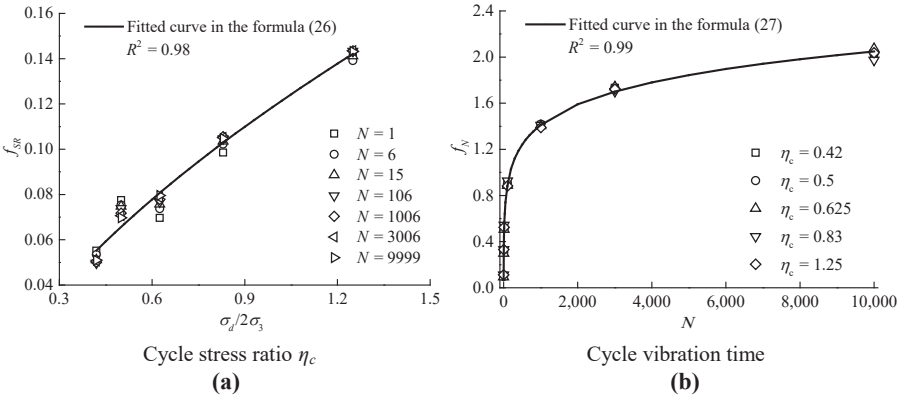

Figure 8.
Correction function of relative grain crushing rate

Table 1 shows the specific values of the fitting coefficients of formulas (26) and (27) for the correction function of relative grain crushing rate.

Other parameters involved in the simulation of the triaxial test of the coarse-grained soil filler of HSR subgrade under cyclic loading can be obtained according to the "trial and error" method. The specific values are shown in Table 2.

Figure 9 shows the cumulative deformation test results and numerical calculation results of the coarse-grained soil filler of HSR subgrade under cyclic loading. It can be seen

Table 1.
Parameter value for correction function of grain crushing rate

Fitting parameters	Fitted value
C_{SR1}	0.16
C_{SR2}	0.58
C_{SR3}	-4.23×10^{-2}
C_{N1}	1.76
C_{N2}	8.16×10^{-2}
C_{N3}	−1.68

from Figure 9 that the calculation results of the cyclic densification model proposed in this paper can more accurately predict different confining pressures and accumulative deformation under stress amplitude but also can accurately predict that the cyclic densification characteristics that the cumulative strain will continue to stabilize as the cumulative vibration time continues to increase. This fully shows that the theoretical formula of the cyclic densification model and the finite element calculation method proposed in this paper are accurate and reasonable.

5. Conclusion

(1) Based on the stress characteristics of long-term repeated low-amplitude cyclic loading of the HSR subgrade, for the coarse-grained soil filler of HSR subgrade, according to the critical state soil mechanics theory, the empirical expressions for grain crushing and plastic work of filler are given, and the shear dilatancy equation of coarse-grained soil filler that can consider the influence of grain crushing and stress ratio is corrected and proposed.

(2) Based on the classical elastic–plastic theory, the correction function of stress ratio and cyclic vibration times is introduced. Through elastic–plastic decoupling, the cyclic densification constitutive model of subgrade coarse-grained soil filler based on the modified shear dilatancy equation is derived.

(3) The numerical analysis and solution program of "elastic prediction–plastic correction" of the proposed model is established. The calculation program is written in FORTRRAN

Source	η_c	η_M	α	μ	δ
Bian *et al.* (2016)	1.00	2.21	0.06	4.5	0.45
Tian *et al.* (2019)	0.42	2.34	1.00	1.5	0.75
Tian *et al.* (2019)	0.83	2.34	1.70	1.2	0.78

Table 2. Parameters of cyclic densification model in numerical implementation

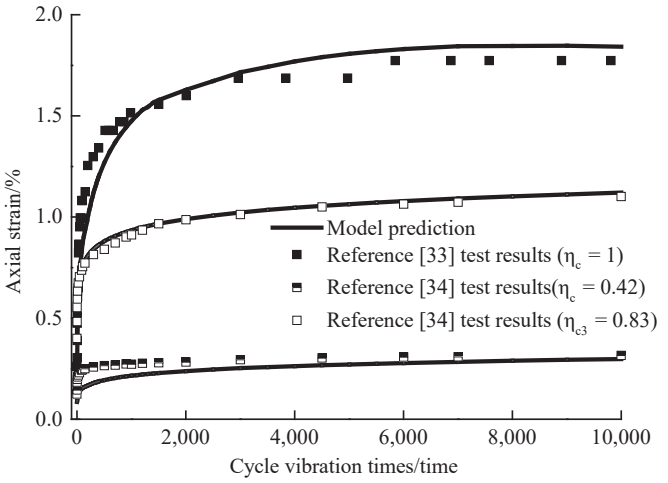

Figure 9. Cumulative axial deformation test results and numerical results of coarse-grained soil filler for the HSR subgrade

language, and the programmed calculation of the constitutive model is realized through the secondary development program interface provided by the finite element software ABAQUS.

(4) Compared with the triaxial test of coarse-grained soil of HSR subgrade under cyclic loading done previously, it shows that the cyclic densification model considering grain crushing proposed in this paper can more accurately simulate the long-term cumulative deformation and cyclic densification characteristics of fillers.

References

Bian, X., Jiang, H., Shen, W., & Chen, Y. (2011). Study on dynamic cumulative deformation of high railway base based on model test. *Journal of Civil Engineering*, *44*(6), 120–127.

Bian, X., Jiang, J., Jin, W., Sun, D., Wei, L., & Li, X. (2016). Cyclic and postcyclic triaxial testing of ballast and subballast. *Journal of Materials in Civil Engineering*, *28*(7), 04016032.1–04016032.11.

Cai, D., Ye, Y., Yan, H., Wei, S., & Yao, J. (2020). Vertical propagation mechanism of vibration wave in intelligent compaction process of high-speed railway subgrade based on field test. *China Railway Science*, *41*(3), 1–10.

Cao, W. (2014). *Secondary Development and Application of Lower Loading Surface Modified Cambridge Model in ABAQUS*. Harbin: Harbin Institute of Technology.

Dafalias, Y., & Popov, E. (1975). A model of nonlinearly hardening materials for complex loading. *Acta Mechanica*, *21*(3), 173–192.

Hardin, B. (1985). Crushing of soil particles. *Journal of Geotechnical Engineering, ASCE*, *111*(10), 1177–1192.

Hardin, B., & Drnevich, V. (1972). Shear modulus and camping in soils: Measurement and parameter effects. *Journal of the Soil Mechanics and Foundation Engineering Division*, *98*(6), 603–624.

Hu, R., Wang, H., & Zhao, G. (2001). Triaxial test of ballast movement. *China Railway Science*, *22*(2), 101–106.

Indraratna, B., Thakur, P., Vinod, J., & Salim, W . (2012). A semi-empirical cyclic densification model for ballast incorporating particle breakage. *International Journal of Geomechanics*, *12*(3), 260–271.

Iwan, D. (1967). On a class of models for the yielding behaviour of continuous and composite systems. *Journal of Applied Mechanics*, *34*(3), 612–617.

Jia, Y., Xu, B., Chi, S., Xiang, B., & Zhou, Z. (2017). Research on the particle breakage of rockfill materials during triaxial tests. *International Journal of Geomechanics*, *17*(10), 04017085.1–04017085.11.

Liu, M., Xie, B., Gao, Y., & Zhan, X. (2013). Simulation of cumulative residual deformation of subgrade soil under long-term cyclic load. *Journal of Civil Engineering*, *46*(10), 135–142.

Mei, H., Leng, W., Liu, W., Nie, R., & Xu, X. (2017). Experimental study on cumulative plastic strain of coarse soil filling in foundation bed under continuous dynamic load. *Journal of the China Railway Society*, *39*(2), 122–129.

Morz, Z. (1967). On the description of anisotropic work hardening. *Journal of the Mechanics and Physics of Solids*, *15*(3), 163–175.

Ning, G. (2018). *Experimental Study on Dynamic Performance of Cementite-stabilized Gravel base Bed under Repeated Freeze-thaw Conditions*. Shijiazhuang: Shijiazhuang Railway University.

Provest, J. (1978). Anisotropic undrained stress-strain behavior of clays. *Journal of Geotechnical and Geoenvironmental Engineering*, *104*(8), 1075–1090.

Qiu, W., & Zhang, H. (2011). The characteristic curve of surrounding rock regarding post-peak behavior. *China Railway Science*, *32*(3), 63–67.

Ramberg, G., & Osgood, W. (1943). *Description of stress strain curves by three parameters*. Washington: National Advisory Committee for Aeronautics.

Salim, W., & Indraratna, B. (2004). A new elastoplastic constitutive model for coarse granular aggregates incorporating particle breakage. *Canadian Geotechnical Journal*, *41*(41), 657–671.

Tabbaa, A., & Wood, D. (1989). *An Experimentally based 'Bubble' Model for clay : The 3rd International Symposium on Numerical Models in Geomechanics* (pp. 91–99). Pande: Elsevier Science Publishers.

Tian, S. (2014a). *Research on Subgrade Filling and Subgrade Deformation Characteristics of Heavy Load Railway Subgrade in Seasonal Frozen soil Area*. Harbin: Harbin Institute of Technology.

Tian, S. (2014b). Deformation characteristics of fillers and subgrade for heavy haul railway in seasonal frozen region. Harbin Institute of Technology.

Tian, S., Tang, L., Ling, X., Kong, X., Li, S., & Cai, D. (2019). Cyclic behaviour of coarse-grained materials exposed to freeze-thaw cycles: Experimental evidence and evolution model. *Cold Regions Science and Technology*, *167*, 102815.

Wang, H. (2001). Test and study on ballast elasticity and accumulated deformation. *China Railway Science*, *22*(6), 106–110.

Wang, J., & Yao, M. (1994). Numerical simulation of dynamic properties of saturated soft clay. In *Proceedings of the 7th Academic Conference on Soil Mechanics and Basic Engineering, China Society of Civil Engineering*, Xi'an: China Society of Civil Engineering.

Xu, G., Xie, D., & Zheng, Y. (1995). Elastic-plastic simulation of cyclic dynamic stress-strain characteristics of saturated sand soil. *Journal of Geotechnical Engineering*, *17*(2), 1–12.

Yang, Z., Elgamal, A., & Parra, E. (2003). Computational model for cyclic mobility and associated shear deformation. *Journal of Geotechnical and Geoenvironmental Engineering*, *129*(12), 1119–1127.

Ye, Y., Cai, D., Chen, X., Yang, Y., & Chen, F. (2020a). In-situ test study on lateral friction of screw pile composite foundation of high speed railway. *China Railway Science*, *41*(2), 1–10.

Ye, Y., Yan, H., Cai, D., Yao, J., Chen, F., & Geng, L. (2020b). Study on influence of compaction parameters of high-speed railway subgrade on evolution characteristics of vibration wave. *Journal of the China Railway Society*, *42*(5), 120–126.

Zhang, K., & Ling, X. (2016). *Geotechnical Earthquake Engineering and Engineering Vibration*. Beijing: Science Press.

Zhang, X., Zhao, C., Zhai, W., *et al.* (2017). Influence of cyclic loading frequency on accumulated deformation behavior of high-speed railway ballast bed. *China Railway Science*, *38*(1), 1–8.

Zhou, W., Leng, W., Liu, W., Nie, R., Yang, Q., & Zhao, C. (2016). Dynamic characteristics of saturated coarse grained soil under low confining pressure cyclic load and study on the backbone curve model. *Rock and Soil Mechanics*, *37*(2), 415–423.

Zhuang, H., Chen, G., & Zhu, D. (2006). Dynamic viscoplastic memory nested surface constitutive model of soil and its verification. *Journal of Geotechnical Engineering*, *28*(10), 1267–1272.

Zienkiewicz, O., & Morz, Z. (1984). Generalized plasticity formulation and applications to Geomechanics. *Mechanics of Engineering Materials*, *44*(3), 655–680.

Corresponding author
Yangsheng Ye can be contacted at: yysh@rails.cn

For instructions on how to order reprints of this article, please visit our website:
www.emeraldgrouppublishing.com/licensing/reprints.htm
Or contact us for further details: **permissions@emeraldinsight.com**